KASCADE-Grande Limits on the Isotropic Diffuse Gamma-Ray Flux between 100 TeV and 1 EeV

W. D. Apel[1], J. C. Arteaga-Velázquez[2], K. Bekk[1], M. Bertaina[3], J. Blümer[1,4,15], H. Bozdog[1], I. M. Brancus[5], E. Cantoni[3,6,16], A. Chiavassa[3], F. Cossavella[4,17], K. Daumiller[1], V. de Souza[7], F. Di Pierro[3], P. Doll[1], R. Engel[1], Z. Feng[8], D. Fuhrmann[9,18], A. Gherghel-Lascu[5], H. J. Gils[1], R. Glasstetter[9], C. Grupen[10], A. Haungs[1] , D. Heck[1], J. R. Hörandel[11], T. Huege[1], K.-H. Kampert[9], D. Kang[1] , H. O. Klages[1], K. Link[4], P. Łuczak[12], H. J. Mathes[1], H. J. Mayer[1], J. Milke[1], B. Mitrica[5], C. Morello[6], J. Oehlschläger[1], S. Ostapchenko[13], T. Pierog[1], H. Rebel[1], M. Roth[1], H. Schieler[1], S. Schoo[1], F. G. Schröder[1], O. Sima[14], G. Toma[5], G. C. Trinchero[6], H. Ulrich[1], A. Weindl[1], J. Wochele[1], and J. Zabierowski[12]
KASCADE-Grande Collaboration

[1] Institut für Kernphysik, KIT—Karlsruhe Institute of Technology, Germany; donghwa.kang@kit.edu, andreas.haungs@kit.edu
[2] Universidad Michoacana, Inst. Física y Matemáticas, Morelia, Mexico
[3] Dipartimento di Fisica, Università degli Studi di Torino, Italy
[4] Institut für Experimentelle Teilchenphysik, KIT—Karlsruhe Institute of Technology, Germany
[5] Horia Hulubei National Institute of Physics and Nuclear Engineering, Bucharest, Romania
[6] Osservatorio Astrofisico di Torino, INAF Torino, Italy
[7] Universidade de São Paulo, Instituto de Física de São Carlos, Brazil
[8] Institute of High Energy Physics, Beijing, China; fengzy@ihep.ac.cn
[9] Fachbereich Physik, Universität Wuppertal, Germany
[10] Department of Physics, Siegen University, Germany
[11] Dept. of Astrophysics, Radboud University Nijmegen, The Netherlands
[12] National Centre for Nuclear Research, Department of Astrophysics, Lodz, Poland
[13] Frankfurt Institute for Advanced Studies (FIAS), Frankfurt am Main, Germany
[14] Department of Physics, University of Bucharest, Bucharest, Romania

Abstract

KASCADE and KASCADE-Grande were multi-detector installations to measure individual air showers of cosmic rays at ultra-high energy. Based on data sets measured by KASCADE and KASCADE-Grande, 90% C.L. upper limits to the flux of gamma-rays in the primary cosmic ray flux are determined in an energy range of 10^{14}–10^{18} eV. The analysis is performed by selecting air showers with a low muon content as expected for gamma-ray-induced showers compared to air showers induced by energetic nuclei. The best upper limit of the fraction of gamma-rays to the total cosmic ray flux is obtained at 3.7×10^{15} eV with 1.1×10^{-5}. Translated to an absolute gamma-ray flux this sets constraints on some fundamental astrophysical models, such as the distance of sources for at least one of the IceCube neutrino excess models.

Key words: cosmic rays – gamma rays: diffuse background

1. Introduction

High-energy gamma-rays represent a very small but also very important fraction of primary cosmic rays. Their importance derives from the fact that they, unlike the charged particles which constitute the bulk of cosmic ray primaries, are not deflected by interstellar magnetic fields. Hence, their direction of incidence on Earth points back to their origin. Also for the case of non-observation of gamma-rays in a certain energy range, upper limits on the flux provide important information.

In addition, investigations of the Galactic and extragalactic diffuse gamma-ray emission are potentially able to give information about the source and propagation of Galactic cosmic rays. The measured flux of diffuse gamma-rays and its spectrum thus would provide new insights into the acceleration of cosmic rays. High-energy diffuse gamma-rays are the sum of contributions from several components. One is the cascading

products from the collision of cosmic rays with interstellar gas and dust in the disk of the Galaxy (Berezinsky et al. 1993). In this case, the predicted integral intensity is concentrated in the Galactic plane. The other is due to electromagnetic cascades induced by the interaction of ultra-high-energy cosmic rays with the cosmic microwave background radiation (Halzen et al. 1990) and the unresolved point sources in extragalactic astronomical objects (Sigl et al. 1994). In these cases, this results in an isotropic flux of secondary photons. Therefore, measurements of the diffuse isotropic gamma-ray flux might provide information on the ultra-high-energy cosmic ray components. Moreover, this flux would represent a background for experiments searching for the gamma-ray enhancement from the direction of the Galactic disk.

Up to energies well into the GeV region gamma-rays are best observed from quite a number of satellites which have been active during recent decades (Ackermann et al. 2015). But with their limited detector size, typically well below 1 m^2, they run out of statistics at higher energies, due to the steep decrease of intensity of all types of primary cosmic ray particles. Therefore, only ground-based experiments are capable of extending observations to higher energies.

---

[15] Now KIT, Division V—Physics and Mathematics.
[16] Now at: INRIM, Torino, Italy.
[17] Now at: DLR Oberpfaffenhofen, Germany.
[18] Now at: University of Duisburg-Essen, Germany.

Gamma-ray astronomy in the upper GeV and TeV regions has seen a dramatic development over the last decade. This was possible due to the development of the Imaging Atmospheric Cherenkov (IAC) technique (Abramowski et al. 2014). Here, the primary particle is not observed directly, but indirectly via the large number of secondary particles produced by its interactions in the Earth's atmosphere. Most of these are relativistic electrons which emit Cherenkov light since they move faster than the speed of light in air. It has been possible, using this technique, to identify gamma-rays from astronomical objects up to about 100 TeV.

Extending these measurements to higher energies is again hampered by poor statistics. IAC telescopes have an effective acceptance area of several times 10^4 m^2. But their field of view is small, below 5°, and they can only take data in dark and clear nights, which limits their observations to 10%–15% of real time even at the most suitable observation sites. Non-imaging Cherenkov light measurements, like the Tunka-133 experiment (Prosin et al. 2014), provide coverage of larger areas, but are still hampered by the requirement of clear, moonless nights. Therefore, air-shower detectors which measure the charged particles produced by the high-energy primary in the atmosphere have been employed to search for cosmic gamma-rays above 100 TeV. Their angular acceptance is well above 60° and they can take data around the clock.

Extensive air showers are mainly characterized by the total electron number and the total muon number. In general, muons are produced by the decay of charged kaons or pions, which in hadronic showers are produced in nucleus–nucleus interactions, whereas in photon-generated showers only by photo-production processes. The ratio between the cross sections of photoproduction and nucleus–nucleus interaction processes is very small, on the order of $\sim10^{-3}$. Therefore, the usual strategy for searching for primary gamma-rays in extensive air showers is to discriminate gamma-ray primaries from the hadronic background by identifying muon-poor or even muon-less extensive air showers.

This paper presents upper limits on the relative intensity of the gamma-ray component of cosmic rays from the measurements by the KASCADE and KASCADE-Grande experiments. In particular, the results of the original KASCADE experiment are updated by including eight years' more data since the publication in Schatz et al. (2003). For the present results of KASCADE-Grande, nearly five times more data sets of the gamma-ray simulations are used, compared to that for the initial result in Kang et al. (2015a), although the same method of analysis is applied.

Earlier measurements of this kind have claimed that about 1 in 1000 cosmic ray particles are gamma-rays at energies around PeV (Nikolsky et al. 1987). More recent experiments (Aglietta et al. 1996; Chantell et al. 1997) were unable to confirm these results and yielded only upper limits of order 10^{-4} for the gamma-ray fraction at energies from 5.7×10^{14} eV to 5.5×10^{16} eV. Recently, a re-analysis of the Moscow State data (Kalmykov et al. 2013) claimed observation of detected gamma-rays at an energy of around 100 PeV, a claim which is still under discussion (Fomin et al. 2017). We have therefore considered it worthwhile to search the full measurements taken by the cosmic ray experiments KASCADE and its extension KASCADE-Grande for events induced by primary gamma-rays. For the present analysis we have chosen the traditional
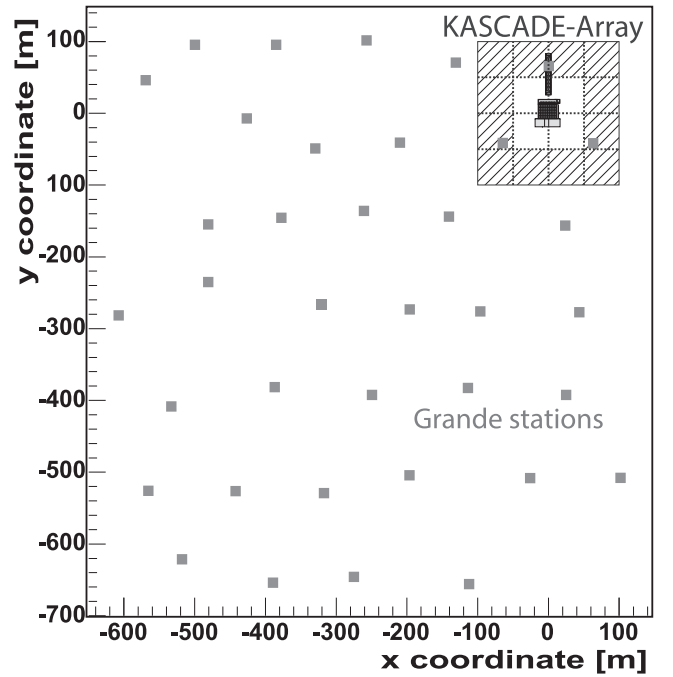

Figure 1. Schematic view of the KASCADE and KASCADE-Grande experiments. The shaded area is covered by 622 m^2 of muon detectors. The KASCADE central detector and muon tunnel are also shown, but not used in this analysis.

method following Helene (1983) in order to compare our results directly with those of earlier studies.

2. Experiments and Data Selection

2.1. The KASCADE Experiment

The KArlsruhe Shower Core and Array DEtector (KAS-CADE) was located at the Karlsruhe Institute of Technology, Germany (8°.4 E, 49°.1 N) at 110 m above sea level, corresponding to an average vertical atmospheric depth of 1022 g cm^{-2}. It operated up to the end of 2012 and all components have been dismantled. The experiment measured the electromagnetic, muonic, and hadronic components of extensive air showers with three major detector systems: a large field array, a muon tracking detector system, and a central detector. A detailed description of the KASCADE experiment can be found in Antoni et al. (2003).

In this analysis, data from the 200×200 m^2 scintillation detector array are used. The 252 detector stations are uniformly spaced on a square grid of 13 m separation. They are organized in 16 electronically independent clusters with 16 stations in the 12 outer clusters and 15 in the four inner clusters (see Figure 1). The stations in the inner and outer clusters contain four and two liquid scintillation detectors, respectively, covering a total area of 490 m^2. In addition, plastic scintillators are mounted below an absorber of 10 cm of lead and 4 cm of iron in the 192 stations of the outer clusters (622 m^2 total area). The absorber corresponds to 20 electromagnetic radiation lengths, representing a threshold for vertical muons of 230 MeV. This configuration allows measurement of the electromagnetic and muonic components of extensive air showers.

Applying an iterative shower reconstruction procedure, the numbers of electrons and muons[19] in a shower are determined basically by maximizing a likelihood function describing the measurements using the Nishimura–Kamata–Greisen (NKG) formula (Greisen 1956; Kamata & Nishimura 1958), assuming a Moliere radius of 89 m. Detector signals are corrected for contributions of other particles, e.g., the signal of the electromagnetic detectors for contributions from muons, secondary gamma-rays, and hadrons (Antoni et al. 2001). The directions of the incoming primary particles are determined without assuming a fixed geometrical shape of the shower front by evaluating the arrival times of the first particle in each detector and the total particle number per station.

In this analysis, to remove from the data set poorly reconstructed showers and to obtain the precise muon number measurement, the following cuts were applied: all of the 16 clusters should be working, shower core positions have to lie inside a circular area of 91 m radius around the center of the KASCADE array to avoid large reconstruction errors at the edges of the detector field, and zenith angles are required to be $\theta < 20°$, where the angular resolution of KASCADE is better than $0°.55$ for electron numbers $\lg(N_e) > 4$. The data set was recorded between 1996 October and 2010 May, which corresponds to an effective time of about 4223.6 days. About 1.0×10^8 events remain for the analysis after the cuts.

2.2. The KASCADE-Grande Experiment

The KASCADE-Grande (Apel et al. 2010) array, covering an area of 700×700 m^2, was an extension of the original KASCADE array and was optimized to measure extensive air showers up to primary energies of 1 EeV (Figure 1). It comprised 37 scintillation detector stations located on a hexagonal grid with an average spacing of 137 m for the measurements of the electromagnetic and muonic shower components. Each of the detector stations was equipped with plastic scintillators covering a total area of 10 m^2. The muon information was taken from the KASCADE muon detectors.

For this analysis, full data sets taken from 2003 to 2012 were used, where only successfully reconstructed and precisely measured events were selected. The core positions of the showers were inside an area of 152,214 m^2 around the center of the Grande array for the same reason as with KASCADE. The zenith angle had to be smaller than $40°$ to ensure full efficiency and an angular resolution better than $0°.5–0°.8$ over the whole energy range. After applying all quality cuts, we obtained in total around 1.7×10^7 events for a measurement time of about 1865 days.

3. Gamma and Cosmic Ray Simulations

An essential part of the present analysis is the Monte Carlo simulation of the shower development and the response of the experiment. Showers initiated by primary photons, protons, He, CNO, Si, and iron nuclei were simulated in order to estimate the mean energies of gamma-rays and cosmic rays, respectively. However, the optimization of the selection of primary gamma candidates is based on the comparison of measured events with simulations of primary gamma-rays, only.

For the simulation of the physical processes in the air shower development the CORSIKA 6.9 (Heck et al. 1998) program was used. To determine the signals in the individual detectors, all secondary particles at the ground level were passed through a complete detector simulation program using the GEANT 3 (Brun et al. 1987) package. The predicted observables at ground level, such as e.g., the number of electrons, muons and photons were then compared to the measurements. The FLUKA 2002.4 (Fassò et al. 2005) model was used for hadronic interactions at low primary energies ($E < 200$ GeV). High-energy interactions were treated with a different model, in our case with QGSJET-II-02 (Ostapchenko 2006). The same number of showers was generated for each particle type. The simulations covered the energy range of $10^{14}–10^{18}$ eV and the zenith angle interval $0°–60°$. The zenith angle distribution followed that of an isotropic flux, where the mean values after considering threshold effects were $12°.7$ and $20°$ for KASCADE and KASCADE-Grande, respectively. The azimuth distribution was flat and uniform over $360°$ for both arrays. The simulations were performed with an E^{-2} spectral index for photons and cosmic rays as well. In total, around 2.5 million events were generated for cosmic rays and also for gamma-rays.

3.1. Estimation of Cosmic Ray Energy

The energy of cosmic rays is estimated from the experimental data. For KASCADE, the formula based on the measurement of the muon and electron numbers of the KASCADE array (Glasstetter et al. 2005) is used. The uncertainties of the energy reconstruction were studied with Monte Carlo simulations. For events of this selection, the typical uncertainty is about 30% for individual events, caused mainly by the unknown cosmic-ray composition.

For KASCADE-Grande, the cosmic ray energy is derived from independent measurements of the charged particles and muon components of the secondary particles of extensive air showers (Apel et al. 2011), where all muon identification comes from KASCADE. The measured data are analyzed on a single-event basis taking into account the correlation of the two observables. The resulting systematic uncertainty in the flux of the cosmic rays is estimated to be 10%–15%, based on the hadronic interaction model QGSJET-II-02.[20]

3.2. Efficiency

To calculate the upper limits of the gamma-ray component of the cosmic ray flux the efficiencies of the experiment have to be known. The trigger and reconstruction efficiency of both experiments is shown in Figure 2. The efficiency is defined by the ratio of the number of reconstructed events in the area compared to the number of simulated events falling in this area, where binomial statistical errors are used. An efficiency greater than one is possible, due to the fact that, from the core uncertainty, eventually more events are reconstructed inside the area than simulated.

For the KASCADE experiment, the trigger and reconstruction efficiency as a function of the shower size, i.e., the number

---

[19] In fact, in KASCADE the so-called truncated muon number is used, which integrates the muon lateral distribution from 40 to 200 m only in order to reduce the effects of electromagnetic punch-through at short distances and the uncertain shape of the lateral distributions at large distances.

[20] It is worth mentioning that there is a difference in the shower muon content of extensive air showers due to effects of the modified treatment of charge exchange processes in pion collisions between the QGSJET-II-02 and the most recent QGSJET-II-04 models (Kang et al. 2013). However, any change in the final results for the present analysis is expected to be negligible as we compare gamma-ray simulations with measured data for the selection of gamma-ray candidate events.
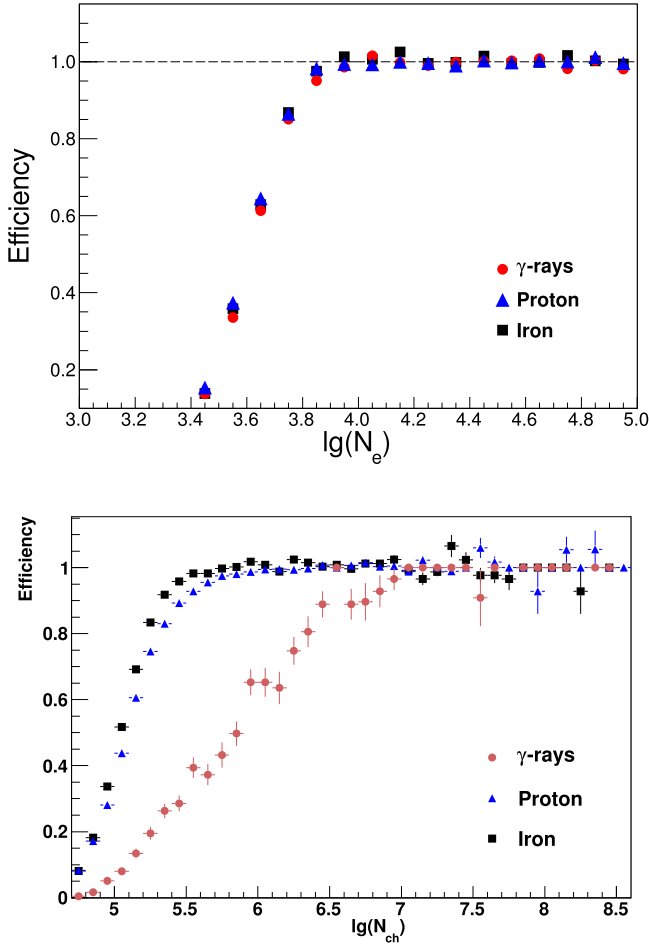
Figure 2. Trigger and reconstruction efficiency as a function of the number of electrons for KASCADE (top) and the number of charged particles for KASCADE-Grande (bottom) for air showers induced by photons, protons, and iron primaries.

Figure 3. Scatter plot of the measured number of muons $\lg(N_{\mu,\mathrm{tr}})$ vs. number of electrons $\lg(N_e)$ for KASCADE (top) and for number of muons $\lg(N_\mu)$ vs. number of charged particles $\lg(N_{\mathrm{ch}})$ for KASCADE-Grande (bottom). In both cases simulated gamma-ray showers are superimposed. The lines indicate the selection criteria for the subset of the muon-poor showers.

of electrons, is demonstrated in the upper graph of Figure 2. The detector array reaches full efficiency on the detection of showers for electron numbers $\lg(N_e) > 4$ for air showers induced by gamma-rays, protons, and iron primary particles, which approximately corresponds to a primary energy of 2.5×10^{14} eV for gamma-rays and 3.3×10^{14} eV for charged cosmic rays.

The trigger and reconstruction efficiency of KASCADE-Grande as a function of the shower size, i.e., the number of charged particles, is demonstrated in the lower graph of Figure 2. Full efficiency is reached at the number of charged particles of around 10^6 for air showers induced by protons and iron primary particles, which corresponds to a primary energy of about 10^{16} eV. However, for showers induced by photon primaries, full efficiency is reached at a higher number of charged particles due to the missing muon trigger at large distances. The limit at high energies is due to the restricted area of the Grande array.

4. Analysis

4.1. Gamma–Hadron Discrimination

Since gamma-ray-induced air showers are notable for their lack of muons compared to hadronic showers, we select a data
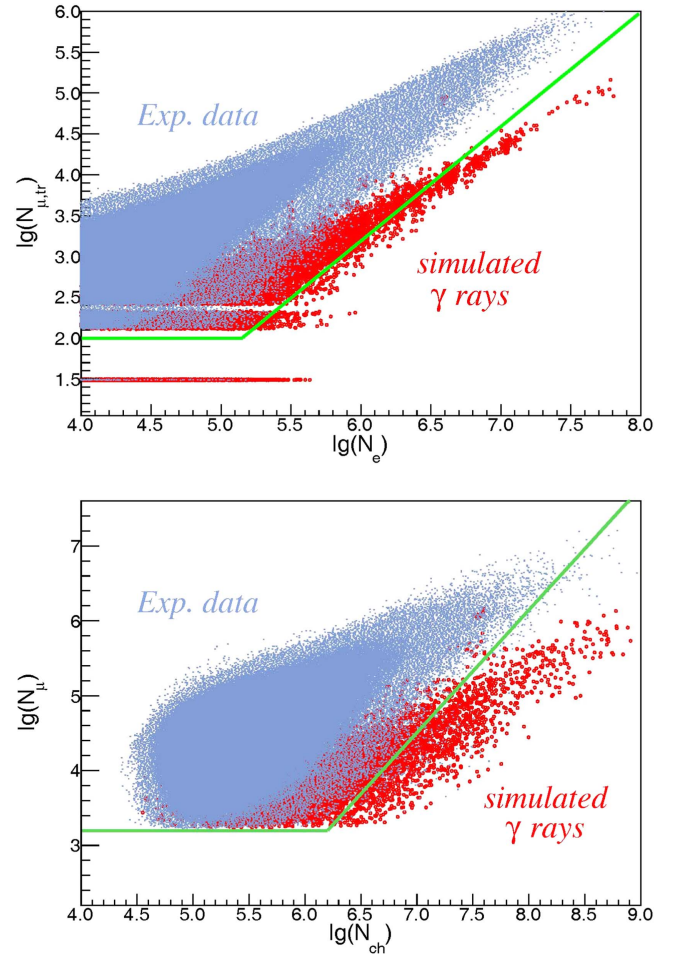
sample enriched in gamma showers by rejecting showers containing muons. Simulations of hadronic air showers underlie large systematic uncertainties due to being above the interaction energies of accelerators and the unknown elemental composition. Therefore, our selection concept is based on using the comparison of the measured events with simulated gamma-ray-induced showers.

The upper graph of Figure 3 shows the distribution of the electron versus truncated muon number $\lg(N_{\mu,\mathrm{tr}}) - \lg(N_e)$ for measured showers by KASCADE with simulated gamma-ray-induced showers. The graph indicates the whole experimental data set, as well as the distribution of the simulated gamma-ray events. Here $N_{\mu,\mathrm{tr}}$ denotes the number of muons in the distance range of 40–200 m from the shower core. The electron number N_e is corrected to a zenith angle of $12°\!\!.7$ using an attenuation length of $\Lambda_{N_e} = 158$ g cm^{-2} (Antoni et al. 2003). In Figure 3, showers without any detected muons are plotted with $\lg(N_{\mu,\mathrm{tr}}) = 1.5$ to be visible on the logarithmic axis.[21] The

---

[21] In KASCADE, it is also possible to detect only one, two, or three muons per shower. When using these low numbers of measured muons to calculate the total muon numbers, almost fixed values are obtained, smeared only by the variation of the core location and the zenith angle of the individual showers (see Figure 3).

Table 1
Results of the Search for Diffuse Ultra-high-energy Gamma-Rays at Different Threshold Values of $\lg(N_e)$ Using KASCADE Data

$\lg(N_e)$	N_{tot}	N_{90}	ϵ_γ	E_{CR}	E_γ	I_γ/I_{CR}	I_γ
>4	1.02×10^8	11653.5	0.33	333	248	$<(2.1 \pm 0.5) \times 10^{-4}$	$<4.02 \times 10^{-13}$
>4.5	2.19×10^7	583.3	0.27	783	605	$<(6.3 \pm 1.5) \times 10^{-5}$	$<2.67 \times 10^{-14}$
>5	3.92×10^6	19.0	0.18	1994	1502	$<(1.7 \pm 0.6) \times 10^{-5}$	$<1.46 \times 10^{-15}$
>5.5	5.76×10^5	2.3	0.20	5247	3673	$<(1.1 \pm 0.8) \times 10^{-5}$	$<1.73 \times 10^{-16}$
>6	6.75×10^4	2.3	0.44	14618	8603	$<(3.1 \pm 2.4) \times 10^{-5}$	$<8.77 \times 10^{-17}$
>6.5	6.66×10^3	2.3	0.94	44952	18610	$<(8.1 \pm 5.8) \times 10^{-5}$	$<4.47 \times 10^{-17}$

Note. The median cosmic ray energy, E_{CR}, and the median gamma-ray energy, E_γ, are given in the fifth and sixth columns, respectively, in units of TeV. The quantities N_{90} and ϵ_γ are defined in the text. I_γ/I_{CR} is the 90% upper confidence limit on the integral gamma-ray fraction with systematic uncertainties, and I_γ is the 90% upper confidence limit on the integral γ-ray flux, in units of photons cm^{-2} s^{-1} sr^{-1}.

distribution of the shower size for gamma-ray-induced showers motivates the following cuts to select the muon-poor showers: $\lg(N_{\mu,\text{tr}}) < 2$ for $\lg(N_e) < 5.15$ and $\lg(N_{\mu,\text{tr}}) < 1.4 \cdot \lg(N_e) - 5.21$ for $\lg(N_e) > 5.15$. This selection of the muon-poor showers, i.e., gamma-ray candidates, is indicated by straight lines in Figure 3 (top).

For KASCADE-Grande, the distribution of the observed number of muons $\lg(N_\mu)$ versus the charged particles $\lg(N_{\text{ch}})$ is shown in the lower graph of Figure 3, where there was never any detection of zero muons.[22] The simulated gamma-ray showers are superimposed as well. Attenuation of the shower size through the atmosphere is corrected to a zenith angle of 20° using the method of constant intensity cut (Apel et al. 2012). The selection of muon-poor showers is indicated by the straight line in Figure 3 (bottom): $\lg(N_\mu) < 3.2$ for $\lg(N_{\text{ch}}) < 6.2$ and $\lg(N_\mu) < 1.64 \cdot \lg(N_{\text{ch}}) - 6.95$ for $\lg(N_{\text{ch}}) > 6.2$.

The stringent selection cuts are motivated by the simulated gamma-rays and their optimization was investigated by changing the slope of the selection line. The cut values were found and optimized by Monte Carlo simulations in order to maximize the purity/efficiency ratio of gamma-ray-induced events. The events below the straight line were taken into consideration for further analysis. They amount to 1056 out of a total of 17 millions events in the case of KASCADE-Grande and to 12,087 out of 100 millions in the case of KASCADE. In the region below this line the events are expected to be mainly due to primary gammas because air showers induced by heavy nuclei show a larger muon-to-electron ratio. We therefore use a conservative method of searching for gamma-ray-induced showers in which the expected background is not subtracted from the event number below the selection lines shown in Figure 3.

4.2. Upper Limit of I_γ/I_{CR}

There is no excess of events consistent with a gamma-ray signal seen in the data. Hence, we assume that all events below the selection line are primary gamma-rays and set upper limits on the gamma-ray fraction of the cosmic rays.

To determine an upper limit on the fraction of the gamma-ray with respect to the cosmic ray integral flux, I_γ/I_{CR}, we use

the equation given by Chantell et al. (1997):

$$\frac{I_\gamma}{I_{\text{CR}}} < \frac{N_{90}}{N_{\text{tot}}\,\epsilon_\gamma}\left(\frac{E_{\text{CR}}}{E_\gamma}\right)^{-\beta+1}. \qquad (1)$$

N_{tot} is the total number of events and N_{90} is the 90% C.L. upper limit on the number of detected events, which is estimated by means of the statistical method from Helene (1983). Using the gamma simulations, we estimate the efficiency for gamma-ray detection and reconstruction, ϵ_γ, after applying the selection cuts. E_{CR} and E_γ are the mean energies of cosmic rays and gamma-rays, respectively, which produce the same shower size. β is the spectral index of the integral flux of cosmic rays: $\beta = 2.7$ for $E < 4 \times 10^{15}$ eV and $\beta = 3.0$ for $E > 4 \times 10^{15}$ eV. This means that, to calculate the energy we weight the simulated energy spectra of gamma-ray and cosmic ray showers to $E^{-2.7}$ below and E^{-3} above the knee, assuming the latter is located at 4×10^{15} eV, as indicated by the measurements of Antoni et al. (2005). The mean energies of cosmic rays and gamma-rays are then calculated bin by bin. Gamma-ray primaries produce larger showers than cosmic ray primaries at the same energy. For this reason, to convert fixed shower size to fixed energy of gamma-ray primary, different factors in the equation have to be taken into account with the assumption that both components have the same spectral index.

Contributions to the systematic uncertainties are mainly due to the quality of discrimination of gamma-rays from cosmic rays (i.e., the statistics of the gamma-ray simulations), the estimation of the cosmic ray energy (i.e., the weighting of the energy spectral index and unknown composition), and the uncertainty in the validity of the hadronic interaction models.

5. Results and Discussion

The results of the search for diffuse ultra-high-energy gamma-rays for different threshold values of N_{ch} are summarized in Tables 1 and 2 for both experiments. Detailed systematic uncertainties on the upper limit of I_γ/I_{CR} are determined and also listed in the tables. We considered here the uncertainties on the energy reconstruction of the cosmic rays and gamma-rays as well as on the slope of the cosmic ray spectrum and the efficiency of the cut. The uncertainties of the estimation of the cosmic ray and gamma-ray energies are estimated to be about 20% (Antoni et al. 2005; Apel et al. 2011) and 10%, respectively. Other sources

---

[22] For KASCADE-Grande showers the muons are measured at larger distances to the shower core at high energies (KASCADE: 40–200 m). In all showers (simulated and measured, gamma-ray or proton induced) at least one muon was detected.

Table 2
Results of the Search for Diffuse Ultra-high-energy Gamma-Rays at Different Threshold Values of N_{ch} Using KASCADE-Grande Data

$\lg(N_{ch})$	N_{tot}	N_{90}	ϵ_γ	E_{CR}	E_γ	I_γ/I_{CR}	I_γ $(\times 10^{-17})$
>6.5	6.19×10^6	358	0.71	3.21×10^4	1.38×10^4	$<(1.88 \pm 0.44) \times 10^{-5}$	<1.19
>7	85537	351	~1.0	8.72×10^4	3.29×10^4	$<(6.79 \pm 1.58) \times 10^{-4}$	<8.51
>7.5	9640	214	~1.0	2.21×10^5	8.30×10^4	$<(2.08 \pm 0.49) \times 10^{-3}$	<8.64
>8	1239	122	~1.0	5.31×10^5	1.98×10^5	$<(1.03 \pm 0.26) \times 10^{-2}$	<8.32
>8.5	165	78	~1.0	1.13×10^5	2.92×10^5	$<(2.48 \pm 0.68) \times 10^{-2}$	<3.89

Note. The mean cosmic ray energy, E_{CR}, and the mean gamma-ray energy, E_γ, are given in the unit of TeV. I_γ/I_{CR} is the 90% upper confidence limit on the integral gamma-ray fraction with systematic uncertainties, and I_γ is the 90% upper confidence limit on the integral gamma-ray flux in units of photons cm^{-2} s^{-1} sr^{-1}.

of systematic uncertainties, like variation of hadronic interaction models or the unknown chemical composition as well as the uncertainties in the slope of the all-particle energy spectrum, are included in these numbers. The error on the efficiency for the gamma-ray detection is evaluated to be smaller than 20%. Thus, the resulting uncertainty is less than 25% in the flux limits, except for the three highest-energy bins of KASCADE, since there the number of events at 90% C.L. is estimated from zero observed events.

To determine upper limits to the integral flux of gamma-rays at fixed gamma-ray energies, we use measurements of the all-particle primary energy spectra reported in Antoni et al. (2005) and Apel et al. (2011). The limits on the gamma-ray flux I_γ are also listed in Tables 1 and 2. To obtain the integral flux of gamma-rays, we multiplied the reconstructed all-particle energy spectrum by the fraction of gamma-rays relative to cosmic rays (I_γ/I_{CR}).

Figure 4 displays the measurements on the gamma-ray fraction as a function of the energy, including this work, for the energy range from 10^{14} eV up to 10^{18} eV. The upper limits of the fraction of gamma-rays at 1.5×10^{15} eV and 3.7×10^{15} eV are obtained to be 1.7×10^{-5} and 1.1×10^{-5}, respectively. These are the lowest upper limits to date. In addition, since around 10^{17} eV (Figure 4) not many experiments have reported results, the limits obtained by KASCADE-Grande are of heightened interest. It should be noted that all values in Figure 4 are upper limits, except that from MSU (Fomin et al. 2013, 2014). This positive signal, however, is in conflict with the limits presented here. Also, a further reanalysis of the MSU data does not confirm the positive signal (Fomin et al. 2017).

Figure 5 shows the comparison of integral flux of gamma-rays with previous experiments (Aglietta et al. 1996; Chantell et al. 1997). Compared with the earlier obtained limits by KASCADE in 2003 (Schatz et al. 2003) there are some differences, in particular at lower energies. This is accounted for by a more detailed investigation using more parameters (i.e., the lateral slope and the smoothness of the electromagnetic component), which affected mainly the lower energies. In this work we focused on higher energies by applying the same method to the KASCADE and KASCADE-Grande data, where those additional parameters for selecting muon-poor events are not effective. The MSU collaboration (Fomin et al. 2014, 2017) recently presented upper limits on the diffuse gamma-ray flux for primary energies around 10–100 PeV obtained from a reanalysis of their old measurements. They are compatible with the presented KASCADE-Grande limits.
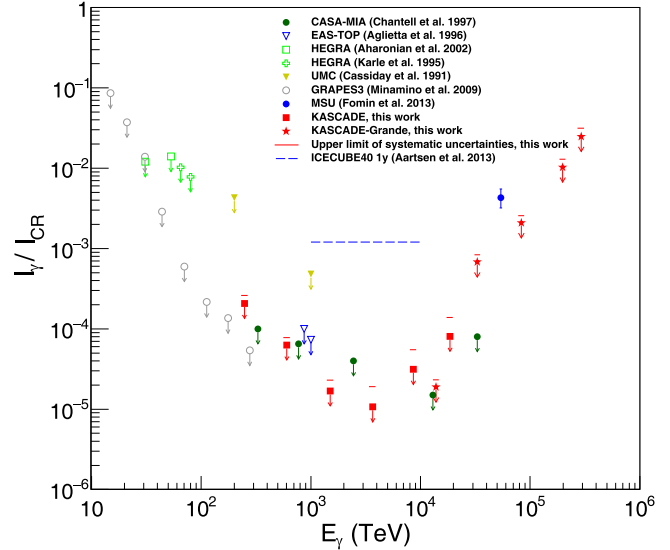

Figure 4. Measurements of the fraction of gamma-rays relative to cosmic rays in the energy range from 10^{13} to 10^{18} eV. The points with arrows represent upper limits from the CASA-MIA (90% C.L., Chantell et al. 1997), EAS-TOP (90% C.L., Aglietta et al. 1996), HEGRA (90% C.L., Karle et al. 1995; Aharonian et al. 2002), UMC (90% C.L., Matthews et al. 1991), GRAPES3 (90% C.L., Minamino et al. 2009), and IceCube (90% C.L., Aartsen et al. 2013), except the MSU (95% C.L., Fomin et al. 2013) experimental value. The red squares and stars represent the results from KASCADE (90% C.L.) and KASCADE-Grande (90% C.L.), respectively, with systematic uncertainties. Limits reported by the Tibet array (3–10 TeV, 90% C.L., Amenomori et al. 2002) and by Milagro (3.5–15 TeV, 90% C.L., Abdo et al. 2008) are out of this energy range.

Figure 5 also compares the exemplary results with theoretical curves using a specific IceCube neutrino excess model assuming proton–proton (pp) interactions and cutoff at 6 PeV (Ahlers & Murase 2014). The lines are the IceCube excess models originating from different distances of neutrino sources in the Galaxy, where these neutrinos are also responsible for primary gamma-rays. The secondary pions from the hadronic interactions of cosmic rays decay at the source and produce a flux of high-energy neutrinos as well as gamma-rays. The relative numbers of neutrinos and gamma-rays depend on the ratio of charged to neutral pions. The flux limits on the gamma-ray flux I_γ of this work at 1.5×10^{15} eV and 3.7×10^{15} eV are lower than the theoretical prediction of the IceCube excess model coming from an 8.5 kpc source distance (dotted black line), which corresponds to the distance from the Galactic center. Therefore, this observation is not in contradiction to the statement that the IceCube excess is associated with extragalactic sources, e.g., gamma-ray bursts or active galactic nuclei. Moreover, there are
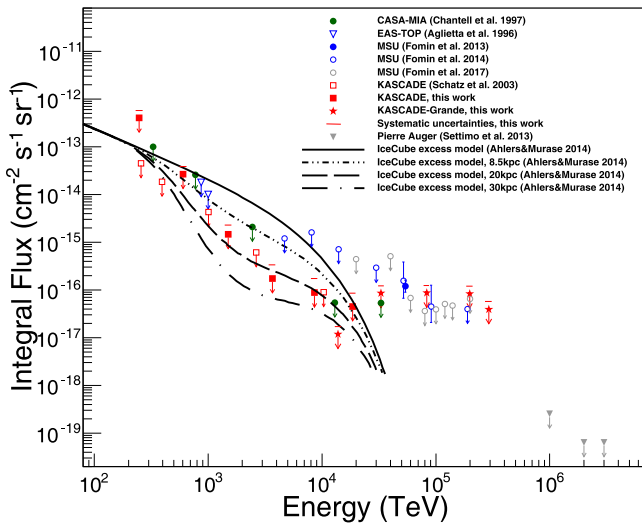
Figure 5. Comparison of integral flux of gamma-rays (including systematic uncertainties) with previous results and with theoretical curves using an IceCube excess model (Ahlers & Murase 2014). The lines are for the unattenuated flux (solid) and that from 8.5 kpc (distance from the Galactic center), 20 kpc, and 30 kpc, respectively. The high-energy points from the Pierre Auger Observatory are taken from Settimo (2013).

other scenarios, e.g., the PeV dark matter decay model in the Galactic halo, suggested to explain the IceCube excess (Ahlers & Murase 2014), which can be additionally constrained by the results of this work, in a similar way as done by Kalashev & Troitsky (2015).

6. Conclusion and Outlook

Using data sets measured by the KASCADE and KASCADE-Grande experiment over a period of 14 and 9 years, respectively, we determined the 90% upper confidence limits to the diffuse flux of ultra-high-energy gamma-rays for the energy range from 10^{14} eV to 10^{18} eV by selecting showers with low muon content.

The upper limit of the fraction of gamma-rays at 1.5×10^{15} eV from the KASCADE measurement is estimated to be 1.7×10^{-5}, while it is 1.1×10^{-5} at 3.7×10^{15} eV. These are currently the lowest upper limits, which were used to set constraints on theoretical predictions, in particular on the distance of sources for the IceCube neutrino excess model (Ahlers & Murase 2014).

By means of the KASCADE-Grande measurements, the best upper limit to the fraction of the gamma-ray to the cosmic-ray flux is obtained: $I_\gamma/I_{\mathrm{CR}} < 1.88 \times 10^{-5}$ for 13.8 PeV. The stringent limits above 100 PeV might constrain a limit to the background rate of muon-poor showers in the search for the Galactic disk enhancement of cosmic rays.

The angular resolutions of KASCADE and KASCADE-Grande are sufficient over the whole energy range to search also for gamma-ray point sources, where a preliminary result was presented in Kang et al. (2015b). However, both analyses will profit from an analysis of combined KASCADE and KASCADE-Grande data, where a coherent shower reconstruction is currently under development. By then, also, an advanced analysis method has to be optimized to give the best results (see, e.g., discussions in Homola & Risse 2007) for such a wide energy range in the search for a diffuse gamma-ray flux.

ORCID iDs

A. Haungs ⓘ https://orcid.org/0000-0002-9638-7574
D. Kang ⓘ https://orcid.org/0000-0002-5149-9767

References

Aartsen, M. G., Abbasi, R., Abdou, Y., et al. 2013, PhRvD, 87, 062002
Abdo, A., Allen, B., Aune, T., et al. 2008, ApJ, 688, 1078
Abramowski, A., Aharonian, F., Ait Benkhali, F., et al. 2014, PhRvD, 90, 122007
Ackermann, M., Ajello, M., Albert, A., et al. 2015, ApJ, 799, 86
Aglietta, M., Alessandro, B., Antonioli, P., et al. 1996, APh, 6, 71
Aharonian, F., Akhperjanian, A. G., Barrio, J. A., et al. 2002, APh, 17, 459
Ahlers, M., & Murase, K. 2014, PhRvD, 90, 023010
Amenomori, M., Ayabe, S., Cui, S. H., et al. 2002, ApJ, 580, 887
Antoni, T., Apel, W. D., Badea, F., et al. 2001, APh, 14, 245
Antoni, T., Apel, W. D., Badea, F., et al. 2003, NIMPA, 513, 490
Antoni, T., Apel, W. D., Badea, F., et al. 2005, APh, 24, 1
Apel, W. D., Arteaga, J. C., Badea, F., et al. 2010, NIMPA, 620, 202
Apel, W. D., Arteaga-Velazquez, J. C., Bekk, K., et al. 2011, PhRvL, 107, 171104
Apel, W. D., Arteaga-Velazquez, J. C., Bekk, K., et al. 2012, APh, 36, 183
Berezinsky, V. S., Gaisser, T. K., Halzen, F., & Stanev, T. 1993, APh, 1, 281
Brun, R., Bruyant, F., Maire, M., McPherson, A. C., & Zanarini, P. 1987, GEANT3 User Guide, CERN/DD/EE/84-1 (Geneva: CERN)
Chantell, M. C., Covault, C. E., Cronin, J. W., et al. 1997, PhRvL, 79, 1805
Fassò, A., et al. 2005, CERN-2005-10, INFN/TC-05/11 SLAC-R-773 (Geneva: CERN)
Fomin, Y. A., Kalmykov, N. N., Kulikov, G. V., Sulakov, V. P., & Troitskiy, S. V. 2013, JETP, 117, 1011
Fomin, Y. A., Kalmykov, N. N., & Karpikov, I. S. 2017, PhRvD, 95, 123011
Fomin, Yu. A., Kalmykov, N. N., Kulikov, G. V., Sulakov, V. P., & Troitskiy, S. V. 2014, JETPL, 100, 699
Glasstetter, R., Antoni, T, Apel, W. D., et al. 2005, Proc. ICRC, 6, 293
Greisen, K. 1956, Progress in Cosmic Ray Physics, Vol. 3, ed. J. G. Wilson (Amsterdam: North-Holland Publishing)
Halzen, A. F., Protheroe, R. J., Stanev, T., & Vankov, H. P. 1990, PhRvD, 41, 342
Heck, D., Knapp, J., Capdevielle, J. N., Schatz, G., & Thouw, T. 1998, Rep. FZKA 6019, CORSIKA: A Monte Carlo Code to Simulate Extensive Air Showers (Karlsruhe: KIT)
Helene, O. 1983, Nucl. Instr. Meth., 212, 319
Homola, P., & Risse, M. 2007, MPLA, 22, 749
Kalashev, O. E., & Troitsky, S. V. 2015, JETPL, 100, 761
Kalmykov, N. N., Kulikov, G. V., Sulakov, V. P, & Formin, Yu. A. 2013, BRASP, 77, 626
Kamata, K., & Nishimura, J. 1958, PThPS, 6, 93
Kang, D., Apel, W. D., Arteaga-Velazquez, J. C., et al. 2013, Proc. ICRC, 33, 388
Kang, D., Apel, W. D., Arteaga-Velazquez, J. C., et al. 2015a, J. Phys. Conf. Ser., 632, 012013
Kang, D., Feng, Z., Apel, W. D., et al. 2015b, Proc. ICRC, 34, 812
Karle, A., Martinez, S., Plaga, R., et al. 1995, PhLB, 347, 161
Matthews, J., Ciampa, D., Green, K. D., et al. 1991, ApJ, 375, 202
Minamino, M., et al. 2009, Proc. ICRC (Lodz), 1723
Nikolsky, S. I., Stamenov, J. N., & Ushev, S. Z. 1987, JPhG, 13, 883
Ostapchenko, S. S. 2006, PhRvD, 74, 014026
Prosin, V. V., Berezhnev, S. F., Budnev, N. M., et al. 2014, NIMPA, 756, 94
Schatz, G., Feßler, F., Antoni, T., et al. 2003, Proc. ICRC, 4, 2293
Settimo, M. 2013, Proc. Int. Conf. on the Structure & Interactions of the Photons, 20th Workshop on Photon-Photon Collisions (Trieste: PoS), 062
Sigl, G., Schramm, D. N., & Bhattacharjee, P. 1994, APh, 2, 401